



University  
of Southampton

SSSU 133  
ISSN 0140 3818

School of  
Engineering Sciences

*Ship Science*

**AUTOSUB Propulsion System Investigation:  
Characterisation of the Force  
Measurement System**

**CD Fallows**

**Ship Science Report No 133**

**January 2005**

**SSSU 133**  
**ISSN 0140 3818**

**AUTOSUB Propulsion System Investigation:  
Characterisation of the Force  
Measurement System**

**CD Fallows**

**Ship Science Report No 133**

**January 2005**

# **AUTOSUB Propulsion System Investigation**

## **Characterisation of the Force Measurement System**

**University of Southampton**

**School of Engineering Science**

**Ship Science**

**C.D.Fallows**

**Report Number : 133**

**January 2005**

# Contents

1 Introduction.....	3
2 Requirement.....	3
3 Procedure.....	4
4 Description of the system under test.....	5
5 The force measurement system.....	6
6 Forces acting upon the force blocks.....	7
7 Signal characteristics.....	7
8 Identification of sources of noise.....	12
9 Signal Processing.....	19
10 Conclusions.....	25
References.....	26

# CHARACTERISATION OF THE FORCE MEASUREMENT SYSTEM

## 1 Introduction

The force measurement system needs to be characterised for two reasons. The first is applicable to all experiments, namely fulfilment of the requirement that conclusions drawn are based on a specific degree of accuracy with a specified level of confidence. The other is peculiar to the nature of the design of these experiments and is discussed next.

The experiments are required to determine the effect of a large number of factors on hull performance. To do this they have been designed as factorial experiments based on orthogonal arrays. An underpinning assumption of the design of such experiments is that all significant interactions are anticipated and taken into account. Other interaction between factors are assumed to be negligible. However, should there be unexpected interactions, these will manifest themselves as an increase in variance about the mean of the measured results, in the parlance as additional noise. Detection of an increase in noise is indicative of the need to include other factors or interactions. This in turn implies the need to re-design the experiment such that the effect of the unexpected interaction may be measured. However, the noise due to the need to include additional factors will be additional to, and indistinguishable from, the inherent measurement variability, or noise, of the measurement system. If the inherent noise of the system is significant and unknown it could well mask the effect of the unanticipated factors. It is, therefore, critical to the approach taken here that the measurement system is thoroughly characterised.

## 2 Requirement

The need is therefore:

- To quantify the accuracy of the measurement system.
- To identify and quantify the sources of noise within it.

The measured force signal will vary with those parameters of the experiment that are considered to be under control. There will be other variations due to those aspects of the experiment not under control. The objective is to determine the effects of the uncontrolled variation on the total force signal. This will be done by quantifying the total force signal variation in terms of the shape of its distribution, its mean and its variance. We will then be in a position to state the results to a quantified accuracy and thereby demonstrate the confidence with which any conclusions may be drawn.

### **3 Procedure**

Whilst the AUTOSUB model was under construction, an available drag plate was used to investigate the measurement system and possible sources of noise in the recorded force signals. Because the dynamometer was designed to facilitate examination of both the drag plate and the AUTOSUB model, with the same measurement and data logging systems, it is taken that understanding obtained using the plate is transferable to the AUTOSUB investigation. Hence, whilst this Chapter discusses plate results, it is assumed that AUTOSUB results exhibit similar behaviour. Thus, results obtained in collaboration with Murphy, using a unique design of drag plate (Figure 1) (Hearn and Murphy, 2001) are used.

The experimental procedure was as follows:

- The plate was dragged down the tank whilst entirely submerged for the full range of velocities.
- Repeat measurements were made at selected speeds to provide statistically significant samples.
- The distribution of output signal was established both for intra-run signals and for sets of runs.
- Possible sources of noise were identified and each was explored.
- The accuracy of the overall measurement system was quantified by comparing measured values with expected values.

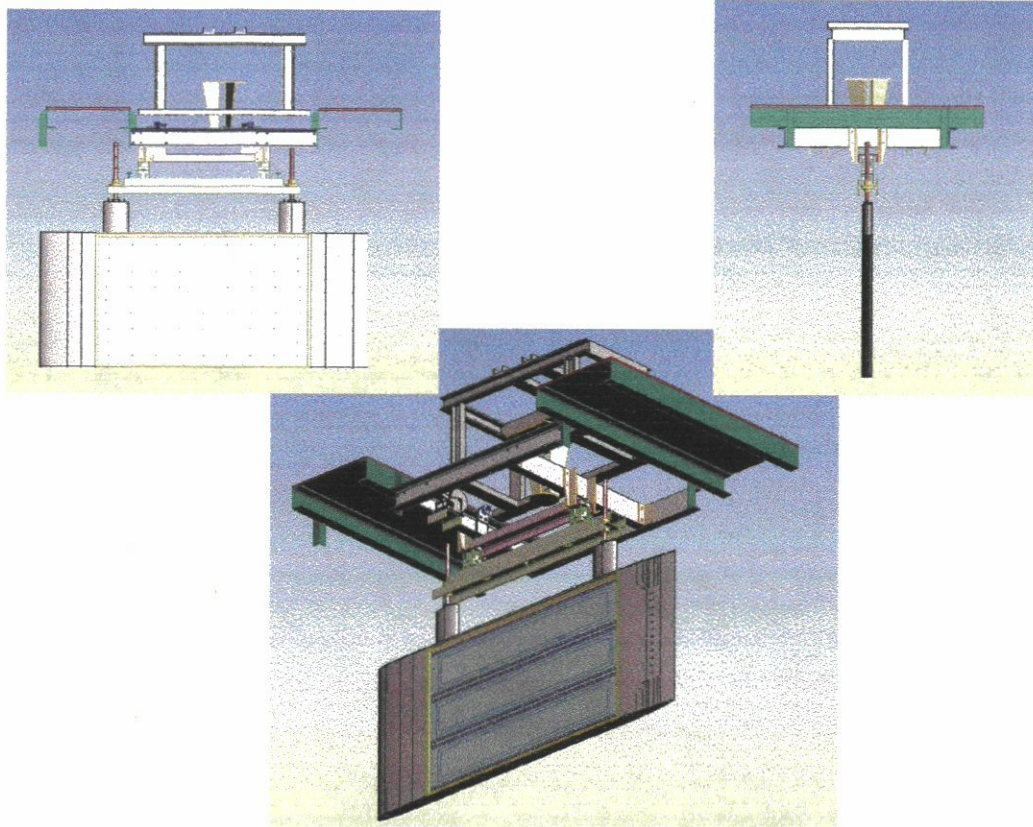


**Figure 1 Drag Plate**

#### **4 Description of the system under test**

The experiment was undertaken in the towing tank described in Section 2.4.3. The plate was mounted in the same manner as that used for the AUTOSUB experiments, i.e. it was mounted to the dynamometer, which in turn was mounted on the carriage. This is illustrated for the model in Figure 2.

The AUTOSUB model (and plate) is entirely passive so no internal forces are generated. The only paths for external transmission of force to the plate are: through the pairs of orthogonal force blocks to each of two mounting posts that apply the motive force to the AUTOSUB model/plate; and through the water in which the plate is immersed.



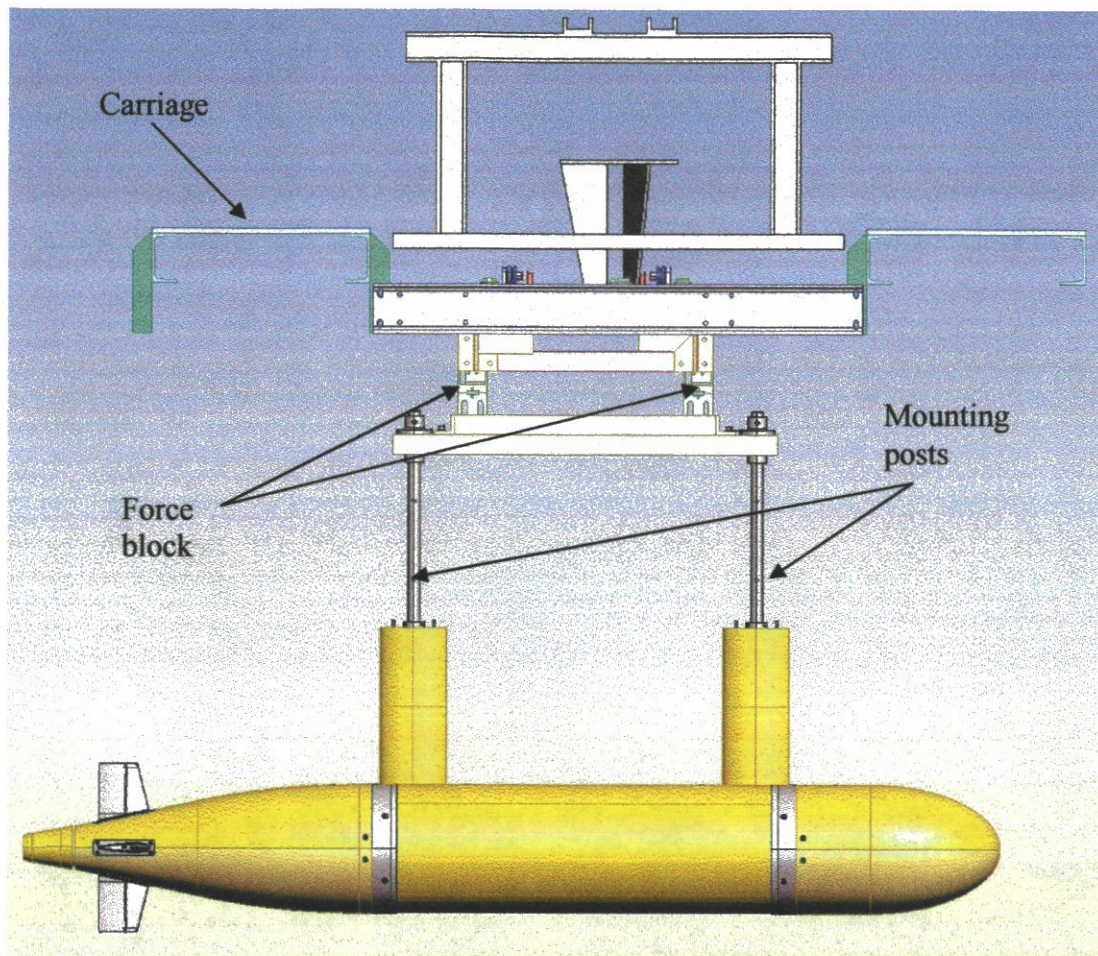


**Figure 2 Model mounting arrangement**

### **5 The force measurement system**

Each force measurement transducer comprises a machined block with force applied between top and bottom surfaces. Transverse displacement is measured by a highly linear (0.09%) LVDT (Linear Variable Differential Transformer) transducer calibrated at 5 kHz. The output from each of the force blocks is amplified and passed through a real time Chebychev analogue filter with 3 switchable options: wide band (no filter), 10 Hz or 1 Hz. The signals are then digitised through an A/D converter and passed to a PC for data logging and display. The sampling rate may be selected as a software function.

The system was calibrated by means of calibrated weights. Amplification of the signal was adjusted to produce maximum discrimination within the range of forces expected



(nominally +/- 200 N). An 11-point calibration curve was obtained by applying forces from 0 to 50 N in 10 N steps in each direction.

The effect of drift in the measurement system was countered by re-setting the zero value at regular intervals. Zero is established by taking the mean of a set of 1000 data points when both the carriage and water are stationary. The value for zero in use for each run is automatically logged. To begin with it was expected that drift would be very low. However, the rate of drift was seen to show considerable variation, so subsequently it was decided to re-set zero between each run. For the experiments undertaken before the policy to re-zero before each run was adopted, the values recorded were adjusted by interpolation between known points.

## **6 Forces acting upon the force blocks**

The possible forces acting on the blocks, and, therefore, included within the recorded data are outlined below.

- Forces generated by the carriage.
  - Propulsion - along the line of the plate
  - Acceleration and deceleration at either end of each run
  - Extraneous noise from:
    - Carriage wheel/rail interactions.
    - Motor – field coil spacing - field excitation pulsing
- Forces generated by the water.
  - Drag
  - Fluctuations due to variation in water kinematic viscosity (temperature).
  - Side forces generated by lift from the plate as a result of imperfect alignment between it and the direction of travel.
- Sympathetic vibration. Any vibrations set up by the above forces may be amplified by:
  - Sympathetic vibrations from the carriage/dynamometer structure
  - Sympathetic vibrations from the plate/mounting post structure.

## **7 Signal characteristics**

The signal received from force block 1 for a typical run is given in Figure 3.

As can be seen, there are large inertial forces at the beginning and end of each run due to the rapid initial acceleration and final braking. For the run used in the above example, the hydrodynamic forces consequent upon travelling at constant velocity are only apparent for the period from 8 to 18 seconds from the start. Consequently data for analysis was only collected for the central sections of runs. An example of such a set of signals from the 4 force blocks is given at Figure 4.

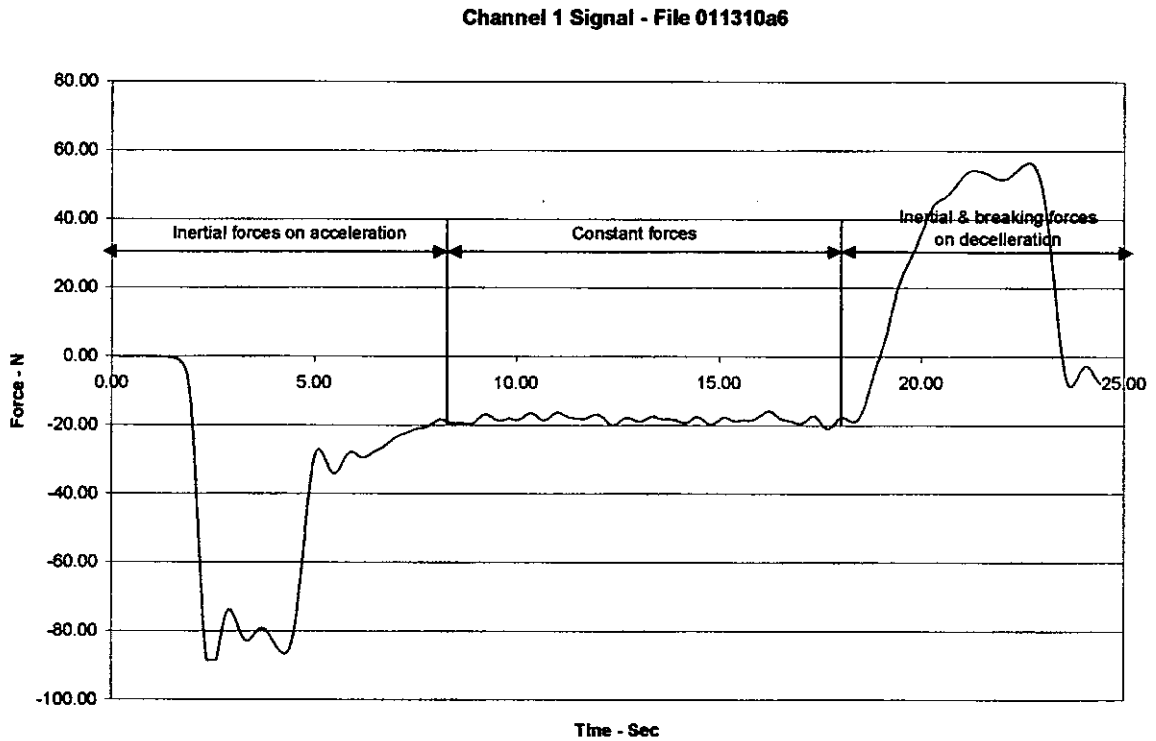


**Figure 3 Typical force block signal**

The signal is noisy with a 5 to 10 N modulation on the basic constant force signals. The records for each individual force signal indicate that, in addition to constant amplitude noise, there are significant transients in the region of 1, 2.5, 4.5 and 7 seconds into the run (Figure 5). The transients appear to be in pairs.

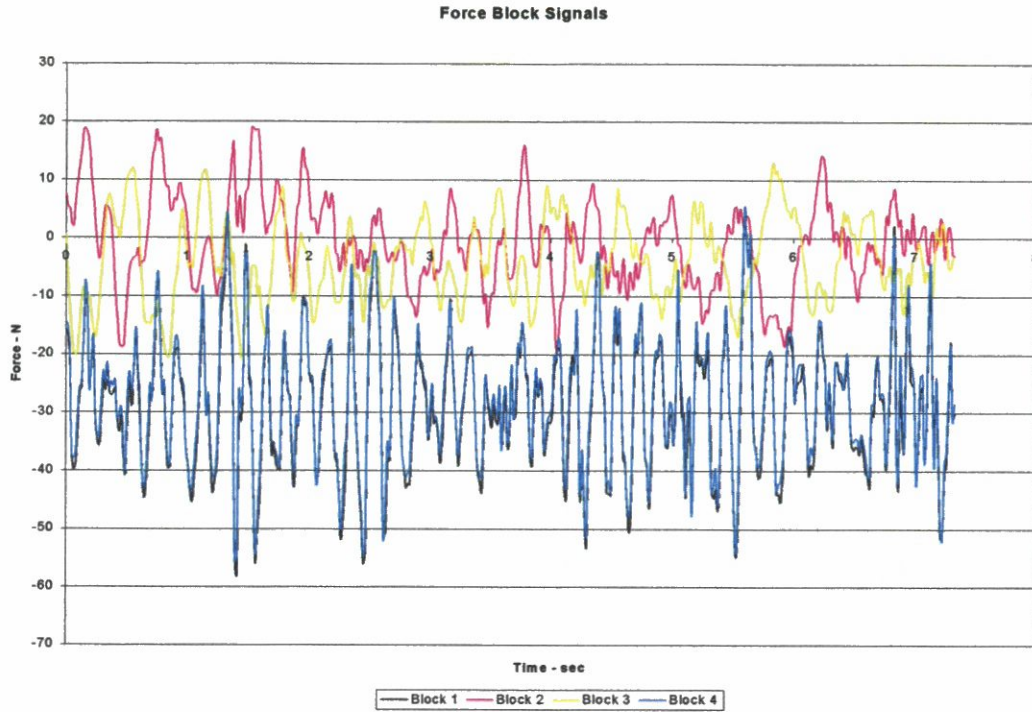


**Figure 4 Signal from 4 force blocks, at constant speed**

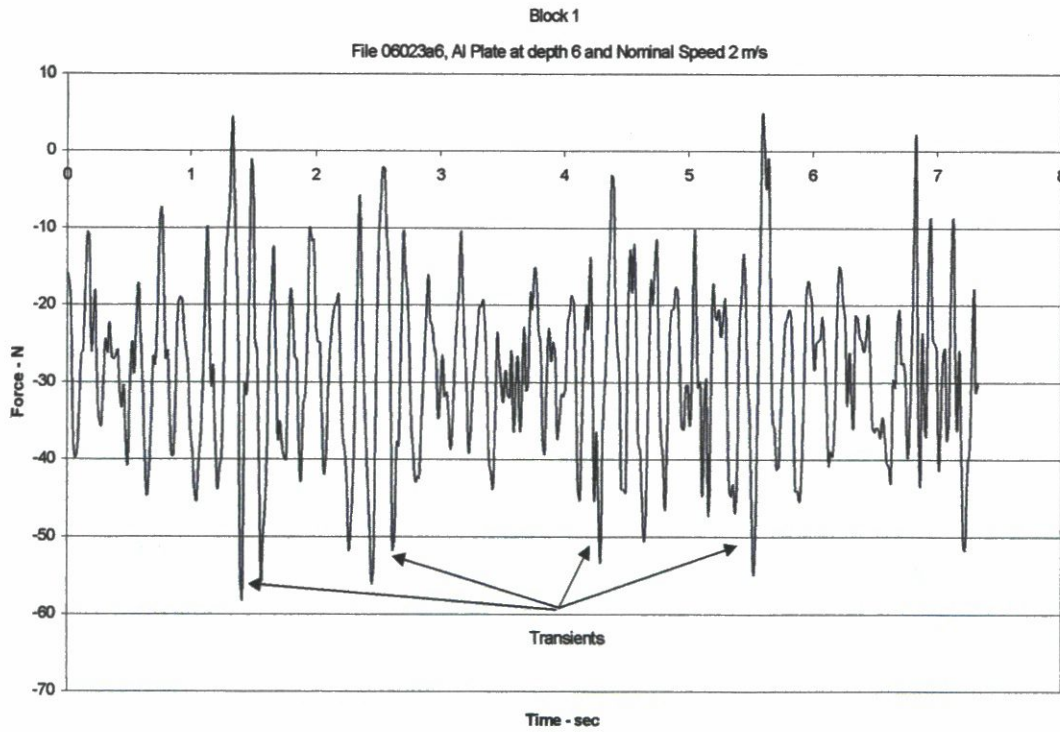


**Figure 5 Force signal transients**

A histogram of the raw signal data from Blocks 1 and 4 is given at Figure 6.

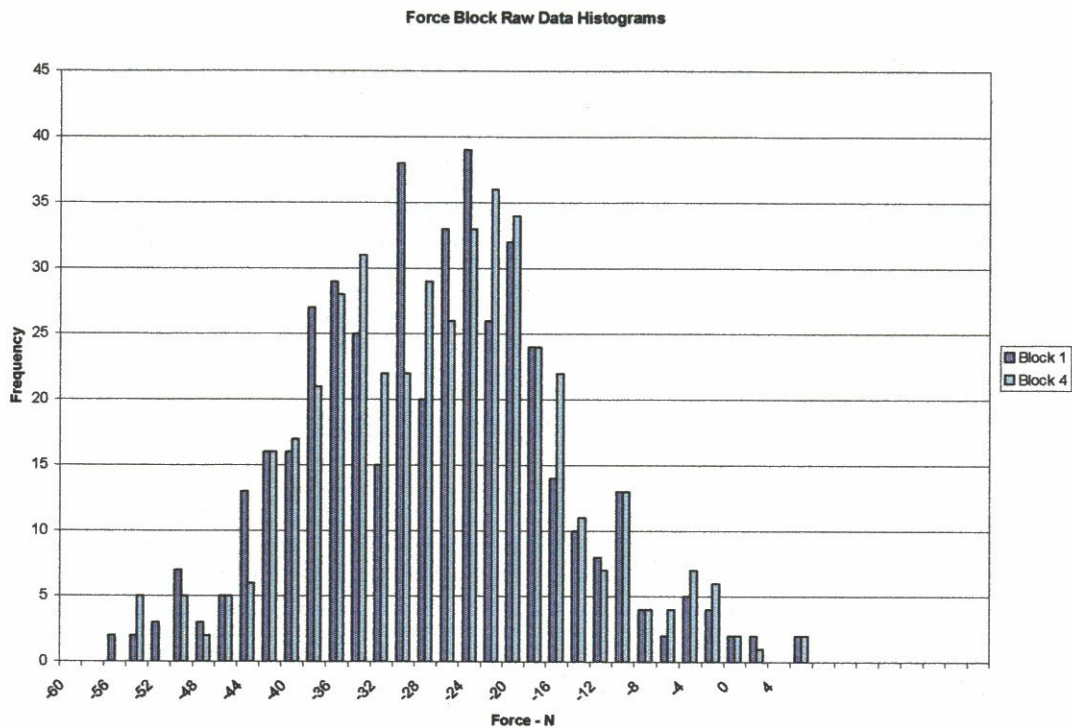


**Figure 6 Histogram of raw force data**

The power spectral density spectra were calculated using Welch's averaged modified periodogram method using a readily available Matlab function. The function operates as follows.

- The time signal is divided into a number of equal sections (in this case 8 with 50% overlap).
- A Hamming window is applied to each section to eliminate the sidelobes that would otherwise be present if a rectangular window had been used. (Fallows, 2005).
- A DFT is applied to the windowed data.
- The (modified) periodogram is computed for each windowed segment. (See (Fallows, 2005) for a description of a periodogram).
- The set of modified periodograms is averaged to form the spectrum estimate.
- The resulting spectrum estimate is scaled to compute the power spectral density by dividing the results by the sampling frequency.

The spectrum from 0 to 10 Hz for Drag Channels 1 and 4 is given at Figure 7 and for Side Force Channels 2 and 3 at Figure 8. The overall power in the spectrum is negligible, but of the power that is generated, peaks occur in the regions of 1-2 and 5-6 Hz.

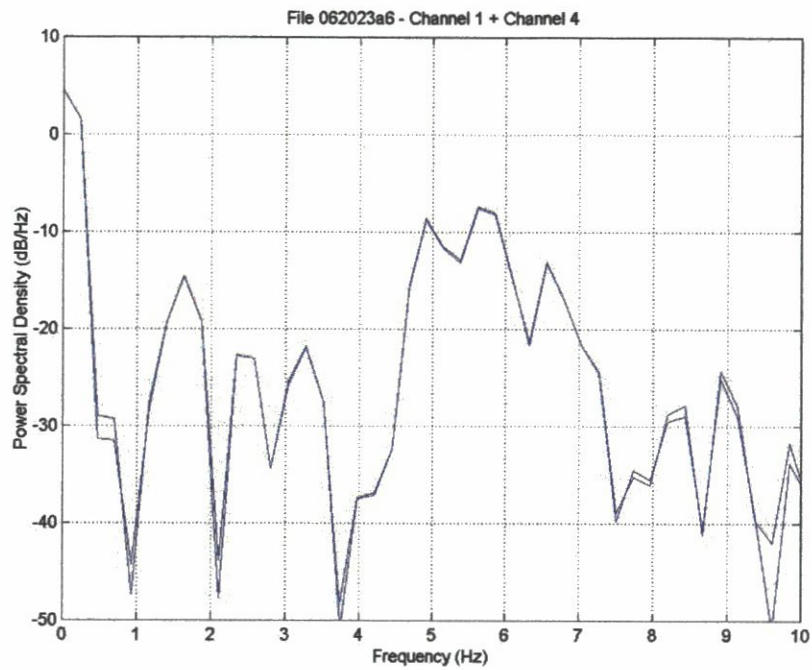


**Figure 7 Frequency spectrum of drag force**

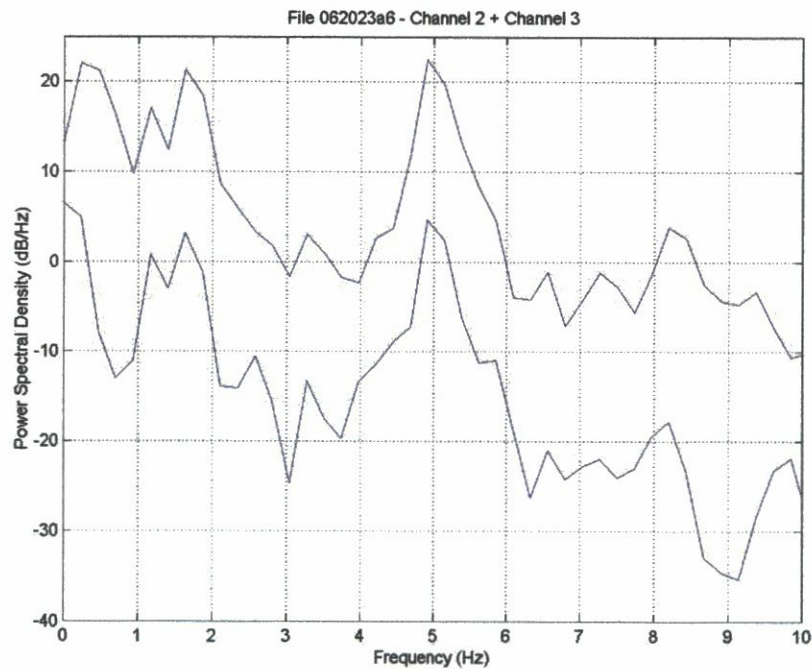


**Figure 8 Frequency spectrum of sway force**

## **8 Identification of sources of noise**

An investigation was undertaken to determine the sources of this noise. The potential contributors include:

- Electrical noise introduced in the measurement system.
- Hydrodynamic noise induced by interaction between the plate and the water.
- Mechanical noise introduced by interactions between the measurement transducers and the plate propulsion mechanism.

### **8.1 Electrical Noise**

The force measurement system was operated in the absence of any input signal, i.e. with the carriage and water stationary. There was no indication of any significant noise.

The effect of real time filtering was explored. A comparison of the signal with and without filtering is given at Figure 9 in the time domain and in Figure 10 as a frequency distribution.

The means between the filtered and unfiltered data differed by 1.2 to 2.7 N (2 to 5 %). It was, therefore, decided to collect all data in wide band mode and post process the data to extract the drag force signal.



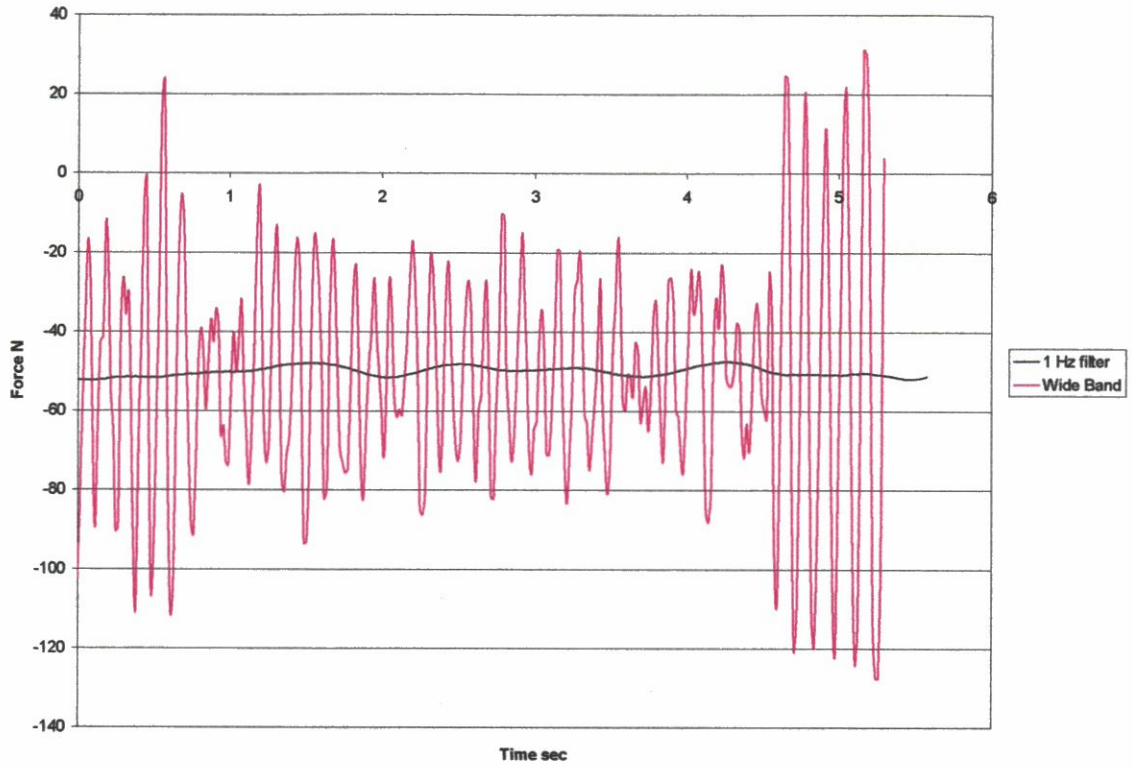


**Figure 9 Effect of filtering in the time domain**

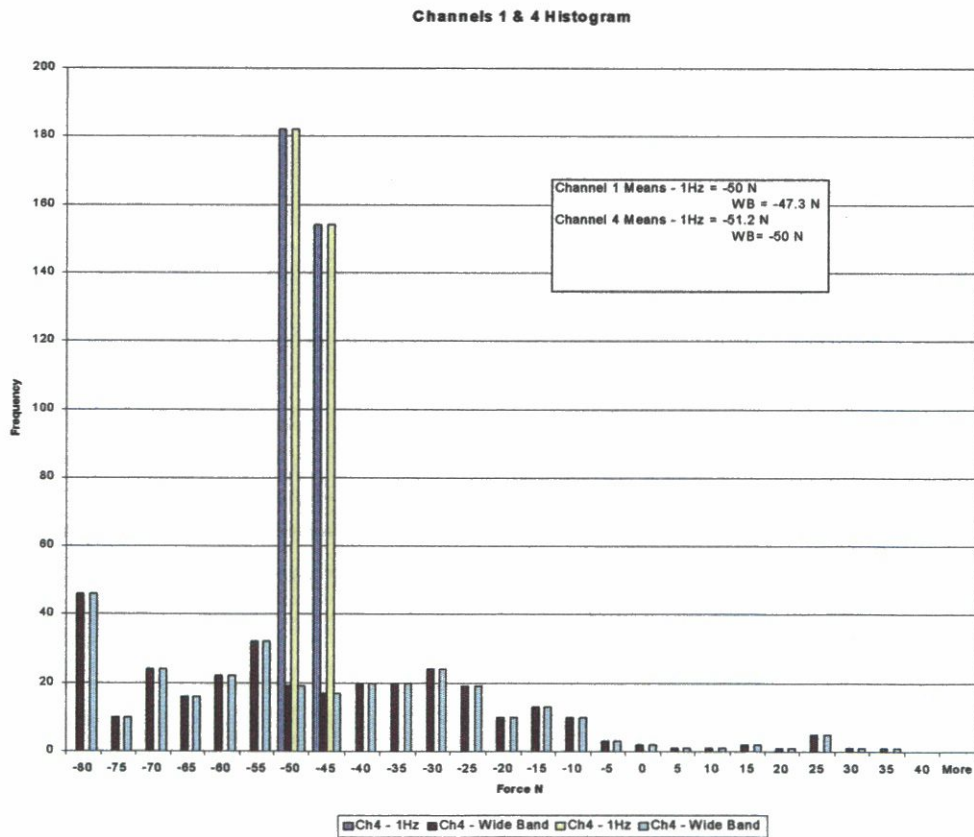


**Figure 10 Effect of filtering in the frequency domain**

## 8.2 Hydrodynamic Noise

The likelihood of noise being induced by means of hydrodynamic forces was investigated. Two possible causes were considered: forces could result from anisotropic water properties such as variations in temperature and density; or result from variations in water pressure due to asymmetric flows round the test plate. The temperature of the water was measured at two depths for each of three positions along the tank during the period of the experiments. No evidence of significant variation was found, either in time or space. Additionally, the density of the water was measured on a number of occasions and positions and there was no evidence of any change.

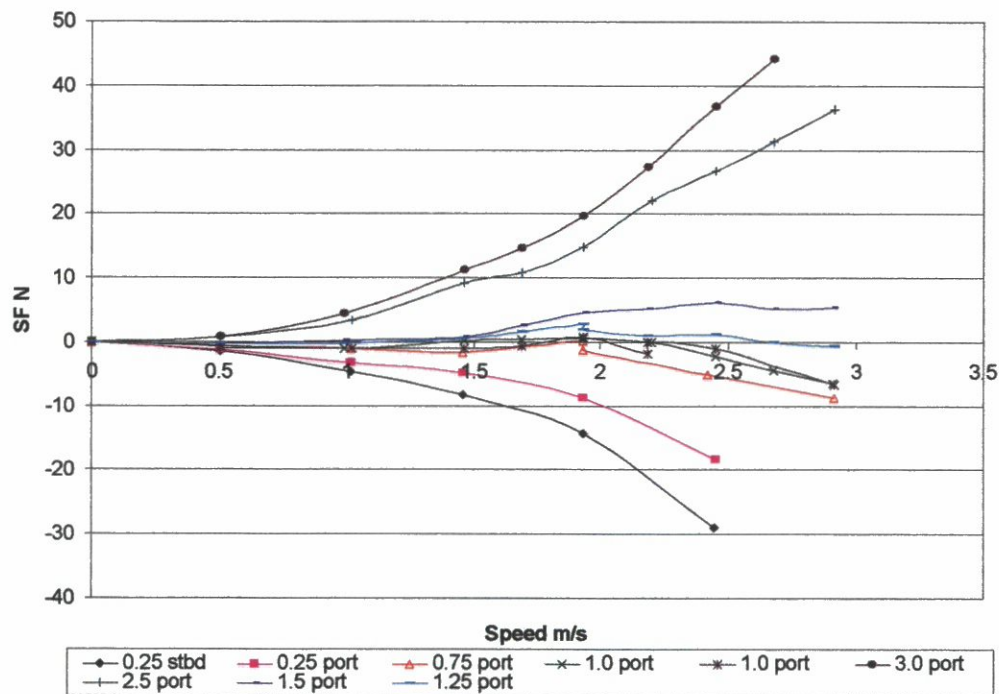


**Figure 11 Plate alignment**

Equally no indication of flow induced noise was found. The test plate had been designed to provide smooth axisymmetric flow (Hearn and Murphy, 2001). It was precisely aligned with the direction of travel. Initial misalignment was detected by measuring transverse force at the forward and after posts. The angle between the plate and direction of travel was then adjusted by means of a micrometer screw until the net side force and yaw moment were minimised as illustrated in the graph at Figure 11.

The plots indicate the net side force as a function of speed for a set number of turns of the micrometer screw from an arbitrary datum point. A similar plot was produced for yaw. Flow visualisation using dye injection confirmed, albeit only at low speeds that symmetrical flow around the plate had been achieved.

### **8.3 Mechanical Noise**

The possibility of noise being generated by the interaction between the wheels and the rails or the wheels and the motor, and this being coupled with the natural modes of oscillation of the mechanical structure was next investigated. The force block signals of the propulsion carriage run with no plate were recorded and characterised. The signal from each channel for the carriage when run un-laden at 2 m/s is given at Figure 12. From these, regular noise can be seen together with the transients observed when the carriage is run with the test plate attached. Knowledge of the carriage speed and the distance between the carriage wheels and between the rail joints enables timing of rail joint/wheel interactions to be calculated. This indicates that the wheel rail interaction is the cause of transients. This is clearly demonstrated in Figure 13, where the wheel and rail spacing is superimposed on the raw signal.

Finally, the response to longitudinal and lateral forces of the plate when attached to the carriage, was investigated. Longitudinal and transverse forces were separately applied to the plate and then abruptly released. The effect of this was to apply a broadband impulse. Analysis of the resultant signals from the force blocks reveals the natural frequencies of the carriage/dynamometer/plate system. An example of the raw signal response of Channel 1, to three applications of force in the transverse directions are shown in Figure 14.

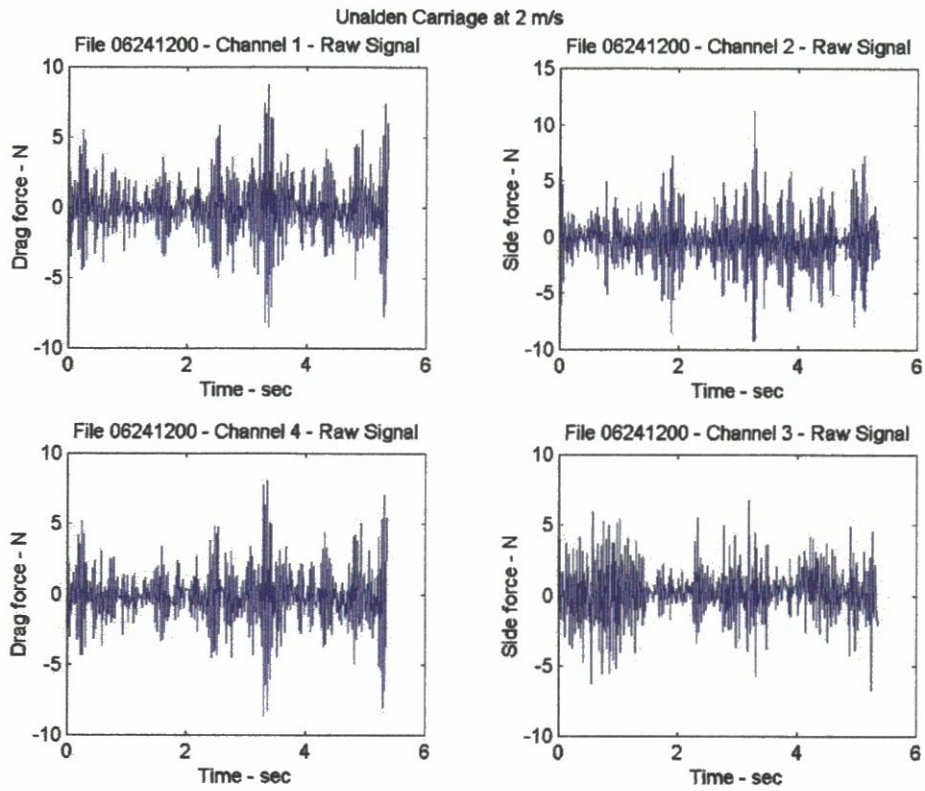


**Figure 12 Force signal. Un-laden carriage**

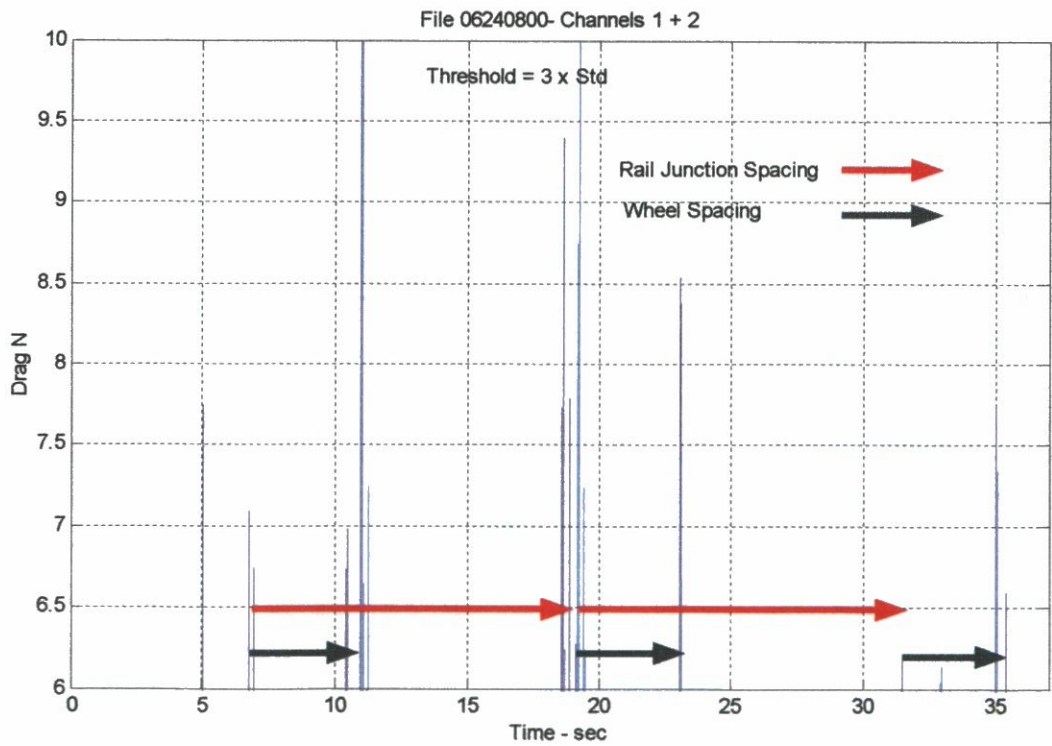


**Figure 13 Force signal noise transients compared with wheel rail events**



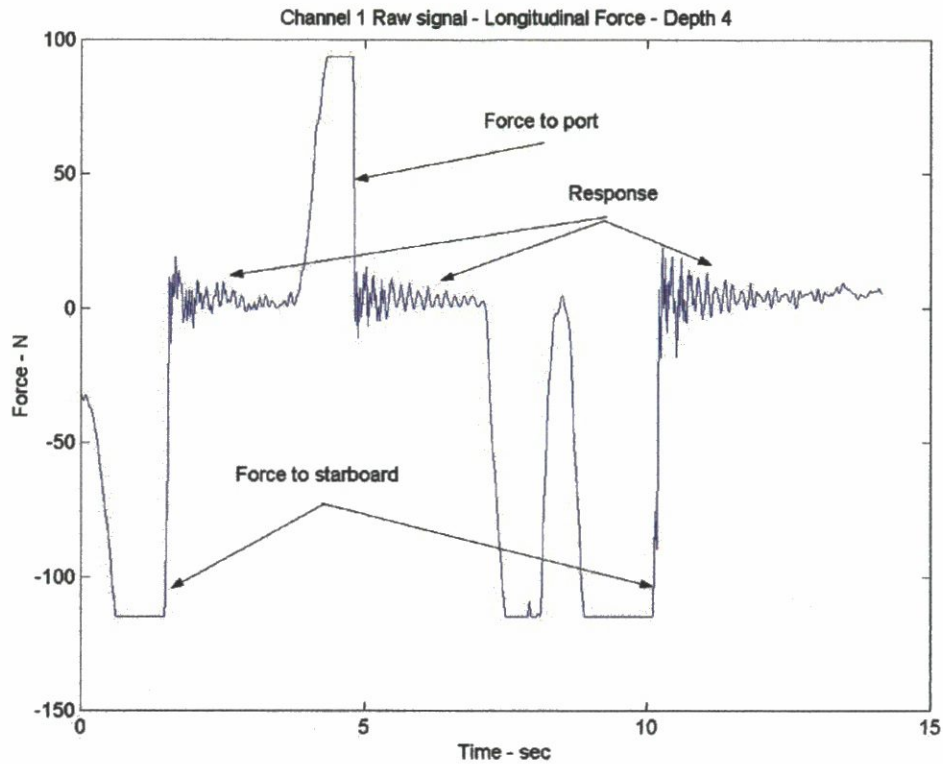


**Figure 14 Response to application of lateral force**

Similar data was collected for applications of force in the longitudinal direction. Data was collected for plate depth settings of 4 and 6. The data was time-sliced to give the response to each application of force and the spectra obtained. Examples of the raw data and spectra are given at Figures 15 and 16. A natural response exists in the region of 6 Hz.

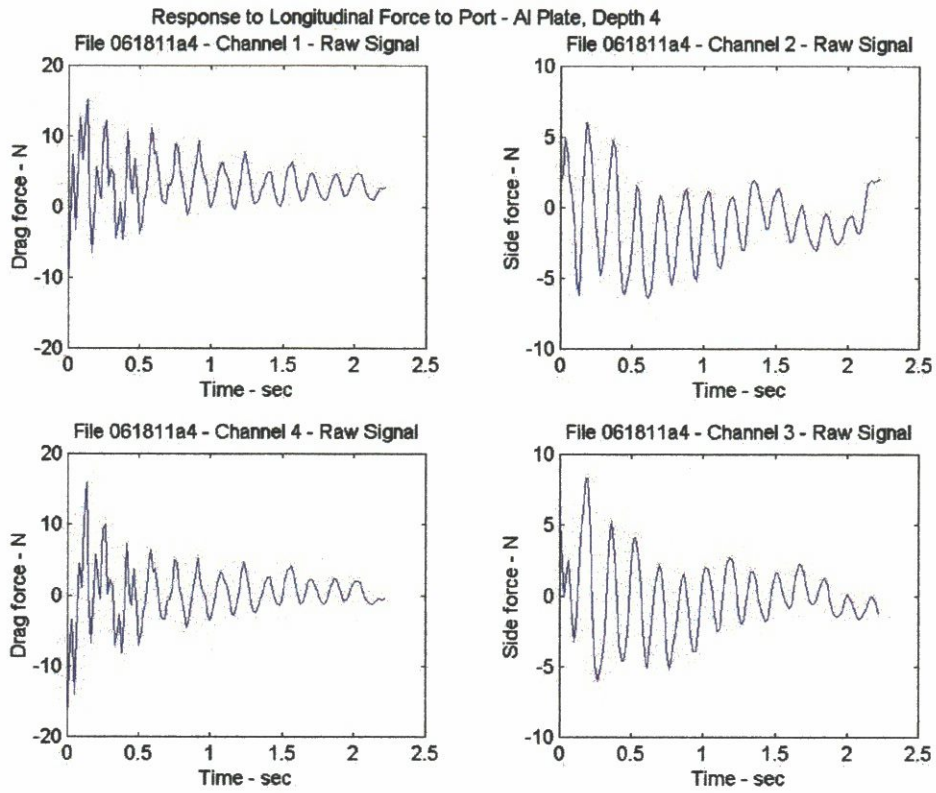


**Figure 15 Time response to applied longitudinal force**

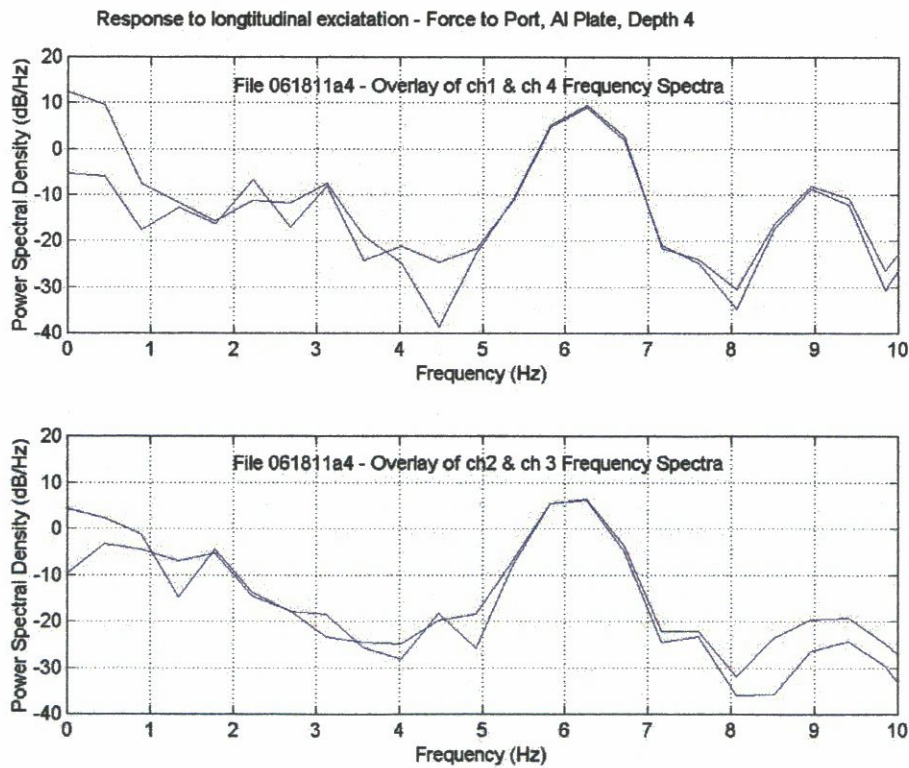


**Figure 16 Frequency response to applied longitudinal force**



It is, therefore, concluded that the plate/dynamometer/carriage assembly has a natural resonance in the region of 6 Hz and that sufficient power is generated by the carriage in this band to induce vibration at this frequency.

## 9 Signal Processing

The data was, therefore, post-processed to remove the induced noise caused by the vibration of the plate, in order to establish its effect on the overall force measurement.

A low pass filter was required with the following specification:

- A pass band (fpass) to 1 Hz.
- Low ripple (Rp) in the pass band.
- A stop band (fstop) from 2 Hz upwards.
- Significant attenuation in the stop band (Rs).

Because processing was to be undertaken on historic data sets rather than in real time, phase response was unimportant since it could be corrected in the processing. Equally, as the data sets were comparatively small (of the order of a thousand records), computational efficiency and processing speed were relatively unimportant.

In general the transfer function of a recursive filter is of the form:

$$\frac{y_n}{x_n} = \frac{a_0 + a_1z^{-1} + a_2z^{-2} + \dots + a_nz^{-n}}{b_0 + b_1z^{-1} + b_2z^{-2} + \dots + b_nz^{-n}}$$

i.e.

$$\frac{y_n}{x_n} = \frac{\sum_{i=0}^n a_i z^{-i}}{\sum_{i=0}^n b_i z^{-i}}$$

where the operator  $z^{-n}$  represents a delay of n sampling intervals, e.g.  $z^{-1}x_n = x_{n-1}$ .

A Chebychev Type 2 IIR (Infinite Impulse Response) filter to meet this specification was designed with  $n = 4$  using the Matlab signal-processing package. This type of filter combines the characteristics of zero in-band ripple and rapid transition to high rejection in the stop band.

Two filters were designed to meet the above requirement but with different rejection band characteristics (-30 dB and -20 dB). Their responses are shown in Figures 17 and 18. The signal from Filter 1, although having a higher rejection band attenuation, was found to settle less rapidly than that of Filter 2. Since the 20 dB rejection level of Filter 2 is more than adequate this was adopted as the basis of post processing.

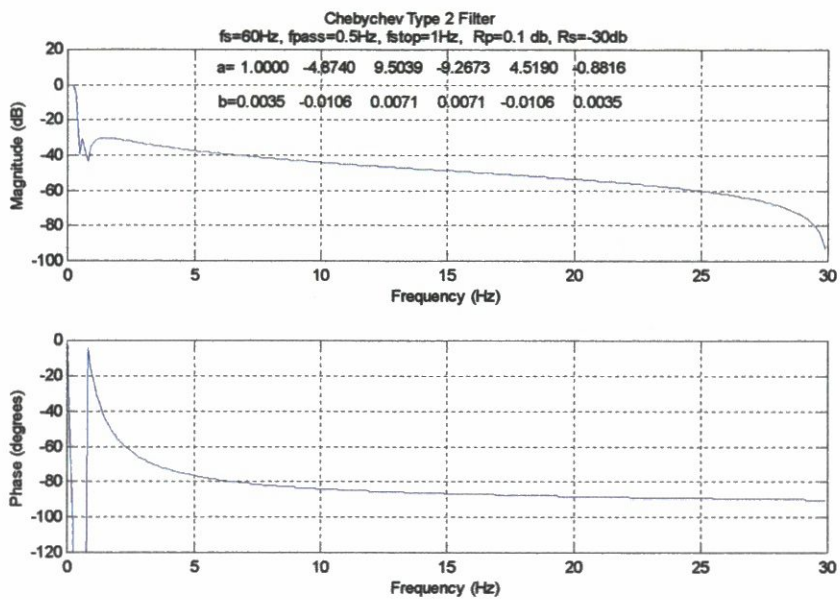


**Figure 17 Filter 1 amplitude and phase response**

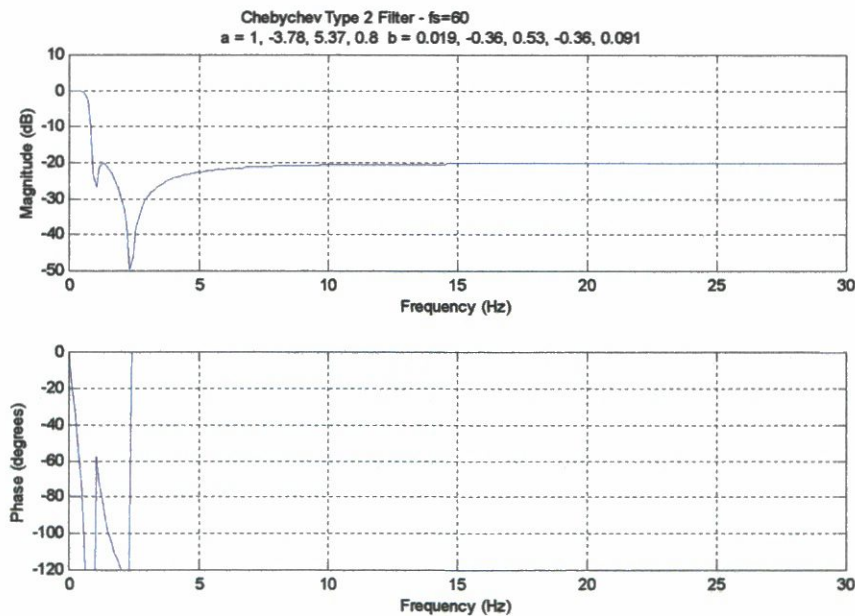


**Figure 18 Filter 2 amplitude and phase response**

The effect of applying this filter to a set of records representative of only the period of constant force is shown at Figure 19. A transient response occurs at the beginning and end of each record. This is due to the nature of the filter used, the characteristics of which, including the indexes, is given at Figure 18. The algorithm used is that of a fourth order recursive filter. It will, therefore, be working on incomplete data sets at the very beginning and end of the process. At both points it will have insufficient data to process and, therefore, at the beginning it will take a number of calculations before the recursive effect settles and at the end it will have no new data whilst the recursive data is still being processed. The post-processed data was, therefore, truncated to remove these transients.

A histogram demonstrating the net effect of the signal processing on a drag and side force signal is shown at Figure 20. This demonstrates that the underlying signal is efficiently extracted from the noise.

AI Plate, Depth 4, Speed 1.46m/s

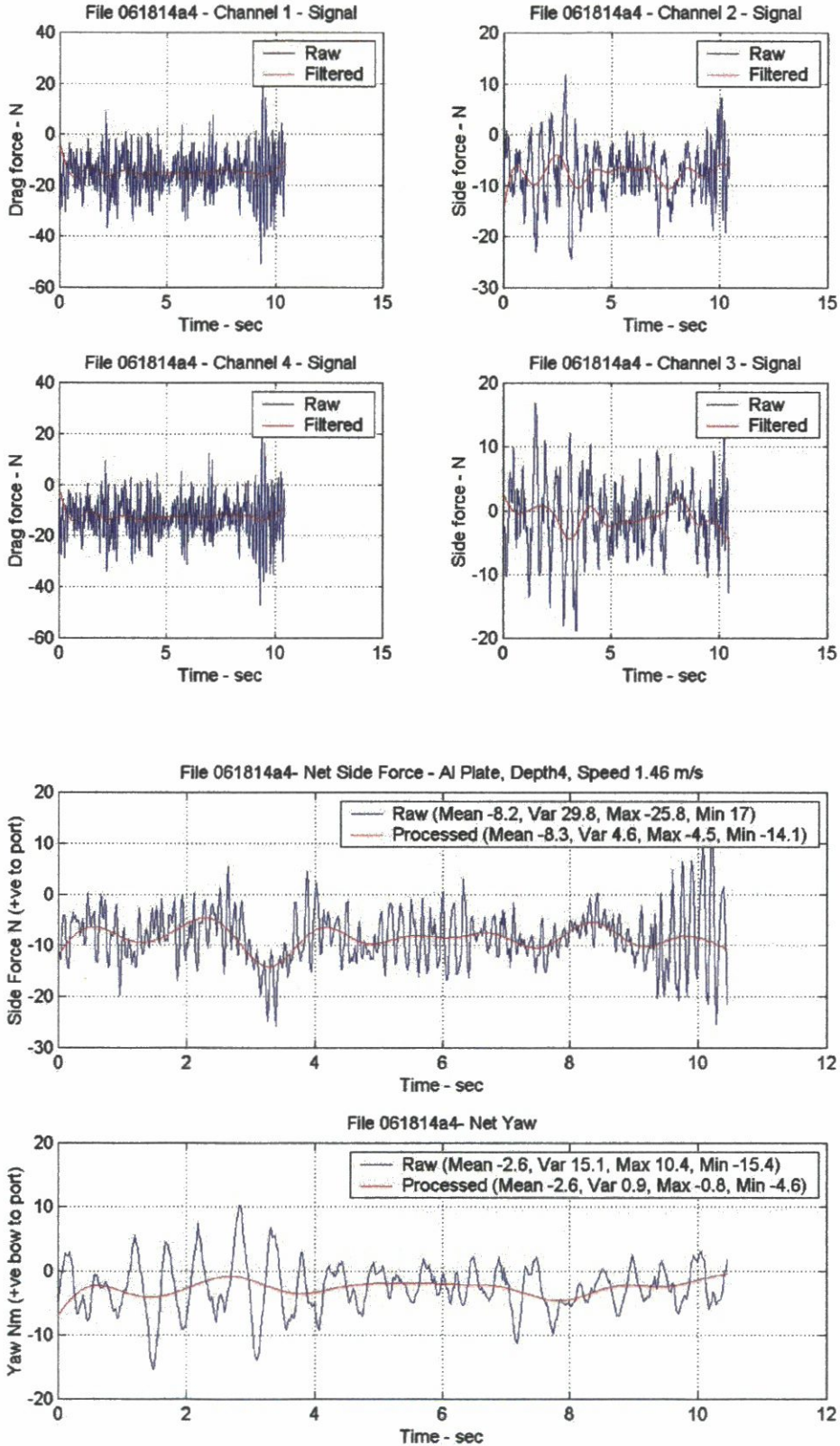
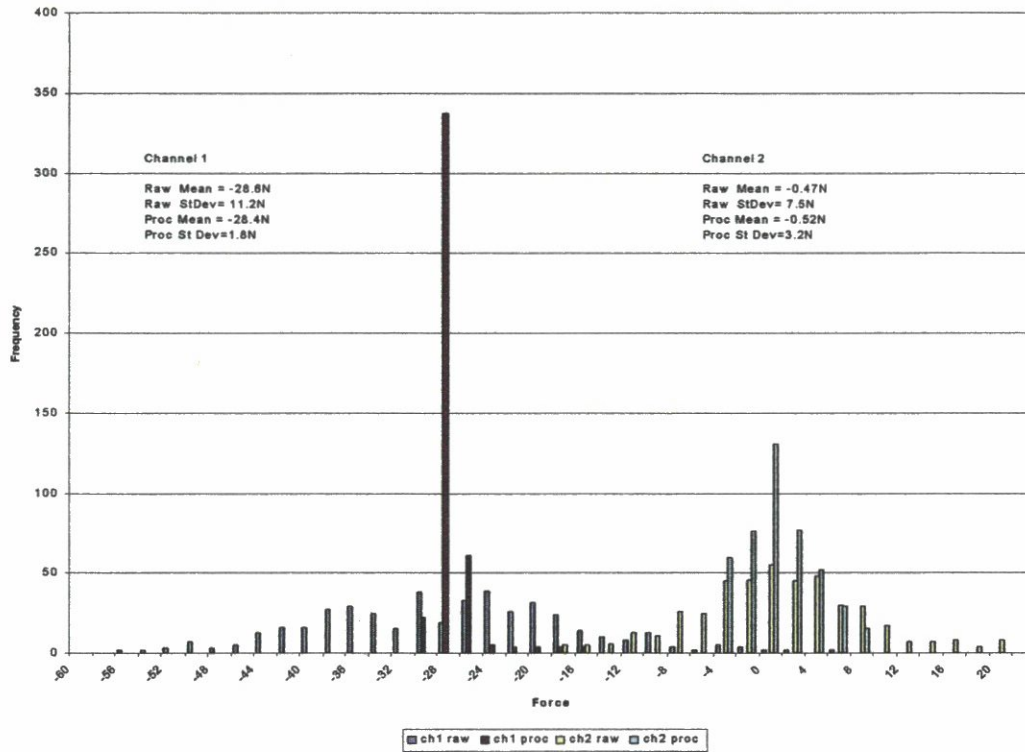


Figure 19 Effect of filtering



**Figure 20 Effect of signal processing**

Some 400 data files, each containing data for 4 force block channels were processed and the statistics of the pre- and post-processed data sets compared. A histogram of the difference between the mean of the raw and processed data for each set is shown at Figure 21. This mean difference between the pre- and post-processed data is 0.06N or 0.018% with a standard deviation of 0.67 N.

The above analysis shows that:

- a. The sources of noise in the force measurement system have been identified and quantified.
- b. An effective means of post processing the data to remove the noise has been developed and demonstrated.
- c. Comparison of pre-and post-processed data indicates that the means of the raw signal provides an accurate indication ( $< \pm 2$  in  $10^4$ ) of the hydrodynamic forces acting on the plate provided that the record contains no inertial forces



such as those associated with acceleration and deceleration of the carriage/dynamometer/model assembly.

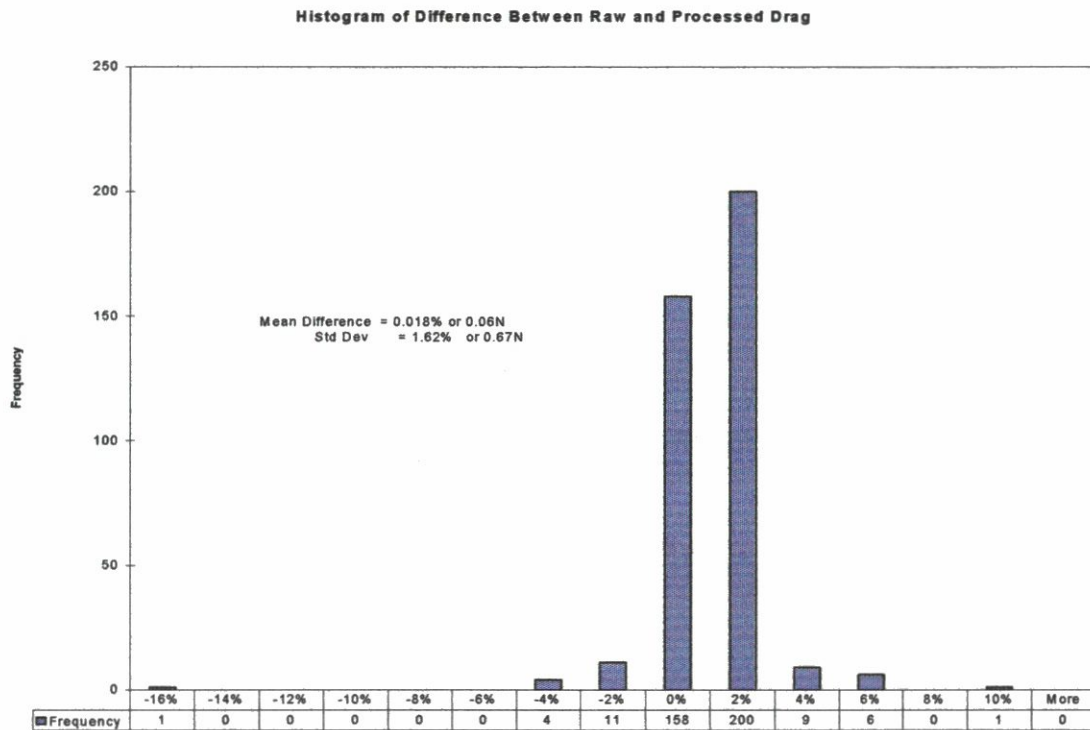


**Figure 21 Difference between raw and processed data**

As a means of testing the data obtained from this investigation as an effective predictor of drag, all of the drag readings obtained at hole depth 6 across a range of speeds is plotted in Figure 22.

The results of a second order polynomial regression analysis shows that the curve follows the expected square law very closely ( $R^2 = 0.9985$ ). The difference between the drag value predicted from this square law and all of the measured values was found to have a mean of 0.006 N with an absolute standard deviation of 0.94 N.



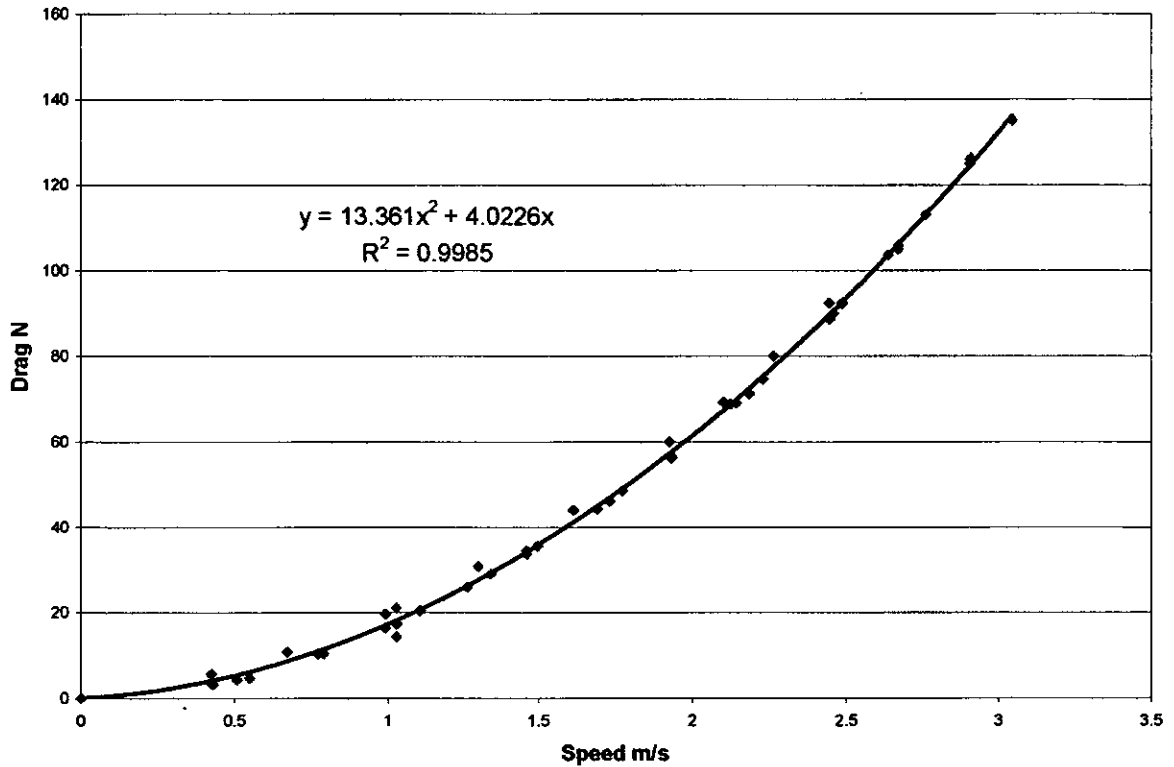


**Figure 22 Drag of plate as function of speed**

## 10 Conclusions

To enable meaningful predictions, it is essential that the measurement system has low and identified noise. The work described in this chapter has identified the causes of all of the detectable sources of noise. None of them produces significant measurement errors.

Assuming that the relationship between speed and drag is a square law, the measurement system has been demonstrated to have a mean measurement accuracy of 0.006N, with a standard deviation of 0.94N.

Given that the AUTOSUB model was prepared using the same NC cutting machinery as was used for the plate, and that the same dynamometer, measuring and logging systems were used in each case, the accuracy limits derived above are considered to be transferable to the AUTOSUB model investigation programme.

## References

- Hearn, G. E. and Murphy, A. (2001), '*Review of Drag Calculations and implications for drag plate design*', University of Southampton, School of Engineering Sciences, Report.
- Fallows, C.D. (2005), '*AUTOSUB Propulsion system investigation - Supplementary information*', University of Southampton, University of Southampton, School of Engineering Sciences, Ship Science, Report 135, pp. 8.